

N. STOJKOVIC¹
M. VASIC¹
M. MARINKOVIC¹
M. RANDJELOVIC¹
M. PURENOVIC¹
P. PUTANOV²
A. ZARUBICA¹

¹Faculty of Science and Mathematics, University of Nis, Nis, Serbia

²Serbian Academy of Sciences and Arts, Belgrade, Serbia

SCIENTIFIC PAPER

UDC 547.216:66.095.21

DOI 10.2298/CICEQ110602062S

A COMPARATIVE STUDY OF *n*-HEXANE ISOMERIZATION OVER SOLID ACIDS CATALYSTS: SULFATED AND PHOSPHATED ZIRCONIA

*Two series of zirconia based catalysts promoted with either sulfates or phosphates were prepared, calcined at different temperatures (600 and 700 °C) and evaluated for the *n*-hexane isomerization reaction. The catalysts with different concentrations of sulfates or phosphates (4 or 10 wt. %) were characterized by BET, XRD and SEM methods, and total acidity was evaluated by using the Hammett indicators. Their final catalytic performances were correlated with their physicochemical properties (surface, structural, textural and morphological). It was found that sulfated zirconia catalyst calcined at lower temperature showed the highest initial activity of all tested catalysts as the result of favorable total acidity, mesopore texture and structural properties. Somewhat lower activity of the sulfated catalyst calcined at higher temperature is related to the content of acid groups partially removed during thermal treatment, thus, lower total acidity, and also to less favorable textural and structural features. Negligible activity of phosphated zirconia catalysts is connected with low total acidity despite the positive status of particular property showing the complexity of the active phase/site formation in the catalyst.*

Keywords: catalyst; isomerization of *n*-hexane; phosphated zirconia; sulfated zirconia.

Recent environmental legislations have introduced strong restrictions on the contents of aromatic hydrocarbons and oxygenated compounds from gasoline characterized by high research octane number (RON) and motor octane number (MON). This consecutively caused newfound need for processes and catalytic materials that would supply high RON and MON without harming the environment. Consequently, the hydro-isomerization of straight chain paraffins has gained importance as one of the main reactions for improving the RON/MON of various fuels [1]. Linear alkanes such as *n*-hexane and *n*-heptane are characterized with octane numbers 25 and 0, respectively, while the (hydro)isomerization reaction would increase the octane numbers to 74 and 45 or even more if multi-branched/di-branched isomers are ob-

tained [2,3]. The economic and industrial viability of the process depends highly on the catalyst used.

Platinum/chlorinated alumina and zeolites have been tested as possible solutions, but failed to satisfy either environmental or economic/process parameters. Namely, the former faces environmental and expense drawbacks, while the latter although proven resistant to impurities does not satisfy due to relatively low activity [4]. That is to say, platinum chlorinated alumina catalyst can be used in the reaction of *n*-alkanes isomerization at low temperatures, *i.e.*, 120–180 °C. However, this catalyst being very sensitive to poisoning and deactivation requires a pre-treatment of the feed. Moreover, chlorine based compounds have to be continuously introduced to maintain the acidity of the catalyst, and consequently its activity. These are reasons why platinum loaded zeolite catalysts that do not show these drawbacks may be also used in commercial isomerization processes [5–7]. Zeolite based catalysts operate at temperatures around 250 °C while at the same time being more resistant to poisons from the feed.

Corresponding author: A. Zarubica, Faculty of Science and Mathematics, University of Nis, 18000 Nis, Serbia.

E-mail: zarubica2000@yahoo.com

Paper received: 2 June, 2011

Paper revised: 19 December, 2011

Paper accepted: 20 December, 2011

In order to obtain more selective catalyst for the production of branched isomers, Pt loaded mazzite was investigated, and proved to be more active for *n*-hexane isomerization under hydrogen pressure than a commercial Pt/mordenite catalyst [5]. Besides, the catalytic performance of the Pt/mordenite catalysts depending on the Pt content for the *n*-hexane isomerization reaction was recently studied, which gave insight into the effect of platinum content [8]. In addition, a series of platinum loaded zeolites (Pt/H β , Pt/HM and Pt/H-ZSM-5) is tested in the *n*-hexane isomerization where the first one showed the best activity and selectivity to isomers [9].

Due to the mentioned drawbacks, a suggestion of a new environmental friendly and active catalytic material with both appropriate structure and strong acidic properties needed to catalyze such a reaction is a challenging task for the near future.

Zirconium oxide (ZrO_2), among other applications, is well known for its favorable catalytic properties. It is used in a wide range of reactions including alkylation, isomerization, biodiesel production, synthesis of 1,5-benzodiazepine and diaryl sulfoxides, benzylation of toluene, etc. [10]. Zirconia is non-corrosive, catalytically active and stable under different conditions. The catalyst may be synthesized in a number of ways, but the sol-gel method is most frequently used nowadays. Zirconia obtained in this manner has highly desirable properties in respect to its nano-sized particles and well resolved porosity. Properties of zirconia based catalysts acquired from the sol-gel method of synthesis depend on a number of parameters: precursor compound, temperature, and pH, solution concentration, aging of sol, solvent type, and promoters used [11].

In order to achieve the surface acidity required for sufficient catalytic activity in isomerization reactions, zirconia may be promoted with acid functions such as sulfates [12] or phosphates. It has been established that zirconia can exist in a number of polymorphs at atmospheric pressure: monoclinic, tetragonal, cubic and orthorhombic [13].

Sulfated zirconia was considered to be a strong solid acid [14]; however, recent studies have shown that the catalyst does not possess super-acidic strength [15]. There is still a controversy on the acidic properties of sulfated zirconia and related activity. Further debate concerned different reactivity of sulfated zirconia catalysts according to the preparation method and activation conditions [16]. Additionally, acid functions have been reported to stabilize the desired tetragonal phase in zirconia [12,13,17,18] for reasons not yet fully understood. Possible explanation ascribes the stabilization to crystal size effect, addi-

tionally connected with the fact that the value of surface energy difference between tetragonal and monoclinic phase surpasses the bulk energy difference between the two phases due to such small size of the particular crystal [10,19,20]. Other authors state that anionic impurities originated from acid modifiers impregnation stabilize the tetragonal phase, and this is the most commonly accepted theory up to date [10,12,14].

Many authors have researched structural properties of a number of sulfated and phosphated zirconia catalysts, obtained in various preparation procedures and under differing conditions [18,21,22], and their activity in isomerization reactions. Alkoxy originated sulfated zirconia was reported to have superior properties compared to the catalyst derived from other precursors, since it retains the preferable tetragonal structure even at higher calcination temperatures [11]. Coupled with the desired phase composition, the catalyst has an appropriate meso-pore size distribution, proven to be beneficial [23].

Over bifunctional metal/acid catalysts the isomerization of *n*-alkanes involves hydrogenation and dehydrogenation steps on the metallic sites (Figure 1, steps 1 and 5), isomerization or cracking steps on the acid sites (Figure 1, steps 2-4) and diffusion steps of the olefinic intermediates from acid to metallic sites and back. It is obvious that the activity and selectivity depend on the characteristics of the acid and metallic sites [8]. When the catalyst is well balanced, the acid function is the limiting one and the product distribution depends essentially on the acidity and pore structure of the solid acid [8].

The aim of this paper is to compare the physical-chemical properties (surface, structural, textural and morphological) of different sulfated and phosphated zirconia catalysts and assess their efficiency in the reaction of *n*-hexane isomerization. To the best of our knowledge, there are no results on the phosphated zirconia catalytic efficiency in the cited test reaction. In addition, the differences of the catalytic performances (activity, selectivity and “life-time”/deactivation) are discussed in light of the registered catalytic features. It is expected that surface and structural properties of catalysts (determined with different acid groups and their content) would influence the final catalytic performances in the test reaction.

EXPERIMENTAL PART

Preparation of catalysts

Zirconia based catalysts were prepared from an alkoxide precursor (zirconium propoxide, 70% solution in 2-propanol, Aldrich Co.) by modified sol-gel

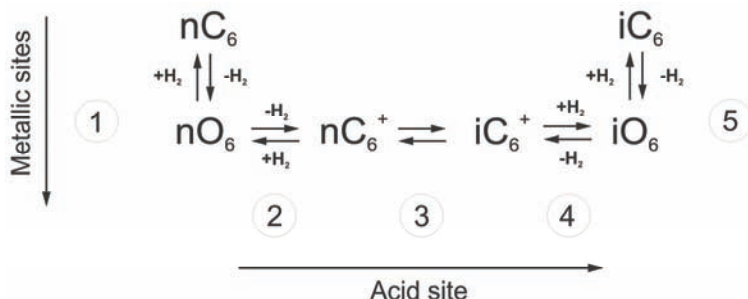


Figure 1. Isomerization of *n*-hexane through bifunctional catalytic mechanism: *n*-C₆ - *n*-hexane; *i*-C₆ - *i*-hexane; *n*-O₆ - *n*-hexene; *i*-O₆ - *i*-hexene; *n*-C₆⁺, *i*-C₆⁺ - carbenium ions [8].

method as reported previously [11]. The sulfating procedure of zirconium hydroxide was done by wet-impregnation using 0.5 M H₂SO₄ for the nominal sulfates content of 4 wt. % (series of sulfated zirconia based catalysts). The introduction of intended 4 or 10 wt. % of phosphates into zirconium hydroxide by using concentrated phosphoric acid was realized in the same way (series of phosphated zirconia based catalysts).

Subsequently, the catalytic samples were then dried and calcined for 3 h in synthetic air flow of 25 cm³/min with a heating rate of 20 °C/min. Both catalysts series were calcined at the two chosen temperatures 600 and 700 °C in order to investigate the thermal treatment influence.

Samples were labeled X-PhZrO₂-Y or X-SZrO₂-Y, where X represented the percentage mass of phosphates or sulfates, Y was the calcination temperature.

Characterization

Basic textural properties of catalytic samples were investigated by low temperature nitrogen adsorption/desorption method using a Micromeritics ASAP 2010. Specific surface areas were calculated using the Brunauer-Emmett-Teller (BET) equation [24]. The pore size distributions (PSD) were calculated by the Barrett-Joyner-Halenda (BJH) method [25]. Desorption branches were used for comparisons. The mean pore diameter was determined as the BJH desorption average pore diameter [21,25]. The pore size distribution curves were additionally plotted by using the computer program [26], and implementing the Kelvin equation [27].

X-ray diffraction analysis (XRD, Philips APD-1700 diffractometer with a Cu-anticathode and monochromator) was used for the determination of the crystal structure of the zirconia based catalysts. The related properties on the total acidity of the catalysts were evaluated by following the color change of Hammett indicators in contact with the surface of the catalysts. The following indicators: *p*-dimethylaminoazobenzene and crystal violet were used covering the range of *H_e* values from 3.3 to 0.8 [28].

Scanning electron microscopy (SEM) was applied in order to obtain data concerning the morphology of the catalyst surface. The scanning electron microscope (JEOL, JSM-6460LV) instrument was used at accelerating voltage of 25 kV, and magnification of 100,000x.

Catalytic tests

Activity and selectivity of catalysts in the reaction of *n*-hexane isomerization were evaluated using a fixed bed micro-reactor under atmospheric pressure and partial *n*-hexane pressure of 60.5 mbar. The reaction conditions were: reaction temperature 300 °C; the molar ratio of He, as the carrier gas, and *n*-hexane was 15.5, and space velocity 6×10⁻² mmol *n*-C₆/g_{cat}·min. The catalysts (0.5 g) were activated *in situ* at the constant temperature of 500 °C in the synthetic air flow of 25 cm³/min during 1 h. The reaction test was carried out for as long as activity was recorded.

Analysis of the reaction products was done by gas chromatography (GC) using an HP Series 5890 II equipped with a flame ionization detector (FID). Injected volume of sample was 0.5 mL. Isomerization products were separated on PONA GC-capillary column (30 m), where 10 cm³/min flow of N₂ was used as carrier gas.

Catalyst selectivity and activity were assessed based on the following calculations:

For conversion:

$$X = \frac{\sum (C_x P_{(H-C)_x} FOD_x) - 6P_{n-C_6} FOD_6}{C - billans} \cdot 100 (\%) \quad (1)$$

where X is the conversion; C_x = 1,2,3,4,5 or 6 - the number of C atoms in a suitable product; P_{(H-C)_x} - total GC peak surface of the products with x C atoms (*n*-hexane, as reactant, was not taken into account here); FOD_x - a detector response factor for a hydrocarbon; C-billans = $\sum C_x P_{(H-C)_x} FOD_x$ - derived by summing the multiplication of the number (x) of C atoms compounds and their total GC peaks surfaces,

multiplied by corresponding response factor - FOD_x (again, *n*-hexane was excluded when calculating *C-billans*).

For total selectivity:

$$S = \frac{\sum(FOD_x P_{x \text{ isomer}})}{FOD_x P_{x \text{ product}}} 100 (\%) \quad (2)$$

where S is the selectivity; $P_{x \text{ isomer}}$ - total GC peaks surfaces of isomers with one and two methyl groups; $P_{x \text{ product}}$ - total GC peaks surfaces of all reaction products (*n*-hexane not included).

For yield:

$$Y_x = X S_x M F \quad (3)$$

where Y is the yield of certain product; X - the conversion; S_x - selectivity of certain product; $M F$ - modified flow in mmol *n*-hexane/g_{cat}·min.

RESULTS AND DISCUSSION

The textural characteristics (BET surface area, BJH cumulative desorption pore volume, average pore diameter and pore size distribution) of all synthesized catalysts are shown in Table 1. These properties are in correlation with the thermal history of the catalysts, type of acidic group incorporated and its content.

The increase of calcination temperature of sulfated and phosphated zirconia-based catalysts has affected the BET surface area decrease to 65 and 41 m²/g, respectively (Table 1) and simultaneously an increase of the average pore diameter. The sintering of the catalytic material operates. Consequently, the average pore diameter becomes higher with the increase of the calcination temperature. Therefore, the sintering process is imposed that probably leads to a consolidation of the catalytic material [11,18,29].

The obtained specific surface areas of the sulfated-catalyst series are 65 and 73 m²/g for the two catalysts calcined at 700 and 600 °C, respectively (Table 1). Literature data for sulfated zirconia catalysts based on zirconium alkoxide precursor prepared with somewhat higher nominal wt. % of sulfate showed

comparable BET surface areas [21] to the analogous ones calculated in the present investigations. To the best of our knowledge, an identical catalyst preparation procedure (all process parameters) compared to ours is not reported elsewhere. Specifically, the authors impose the BET surface area of zirconia-based catalysts should be correlated with the preparation procedure and conditions applied.

It is noticeable that the sulfation procedure did not increase the BET surface area of the modified zirconia much compared to the phosphate introduction in the zirconia-based catalysts synthesized under the same preparation conditions (4-SZrO₂-700 vs. 4-PhZrO₂-700).

Nitrogen isotherms and pore size distributions for sulfated catalysts (4-SZrO₂-600 and 4-SZrO₂-700) are shown in Figure 2. The N₂ isotherms for both catalysts exhibited typical s-shape behavior of type-IV with a type-H1 desorption hysteresis. Both catalysts samples showed a pore system preferably in the mesopores range between 20 and 100 nm with an average pore diameter around 5 nm according to the BJH desorption. The pore size distribution changed only slightly and is shifted towards bigger average pore diameter with increasing the calcination temperature to 700 °C (Figure 2). Two clear maxima in the PSD are observed that may be significant during catalytic run. Namely, the authors have previously shown that the existence of mesopores in contrast to micropores affected the mechanism of slower catalyst deactivation and accordingly longer catalytic life [23]. There is a maximum of the average pore width around 30 nm, and also an additional narrow maximum is observed in the region at the edge of mesopores/micropores dimensions (2.5-3.0 nm). The last mentioned maximum is shifted to slightly bigger mesopores in the case of the catalyst calcined at higher temperature (4-SZrO₂-700) (Figure 2). Thus, the increase of calcination temperature affected the shift of the pore diameters to somewhat higher values for sulfated zirconia-based catalysts.

The BET surface areas of the phosphated series are in the range from 41 to 55 m²/g with the exception

Table 1. Specific surface areas, average pore diameters, pore volumes and maxima in pore size distribution for sulfated and phosphated zirconia catalysts

Catalyst	BET surface area, m ² /g	Average pore diameter, nm	BJH pore volume, cm ³ /g	Maxima in PSD, nm
4 - SZrO ₂ - 600	73	7.2	0.15	2.5; 20-100
4 - SZrO ₂ - 700	65	8.3	0.16	3.0; 20-100
4 - PhZrO ₂ - 600	109	7.6	0.24	3.5; 10-90
4 - PhZrO ₂ - 700	47	10.9	0.15	3.0; 20-75
10 - PhZrO ₂ - 600	55	9.7	0.16	3.0; 20-80
10 - PhZrO ₂ - 700	41	11.2	0.14	3.0; 20-80

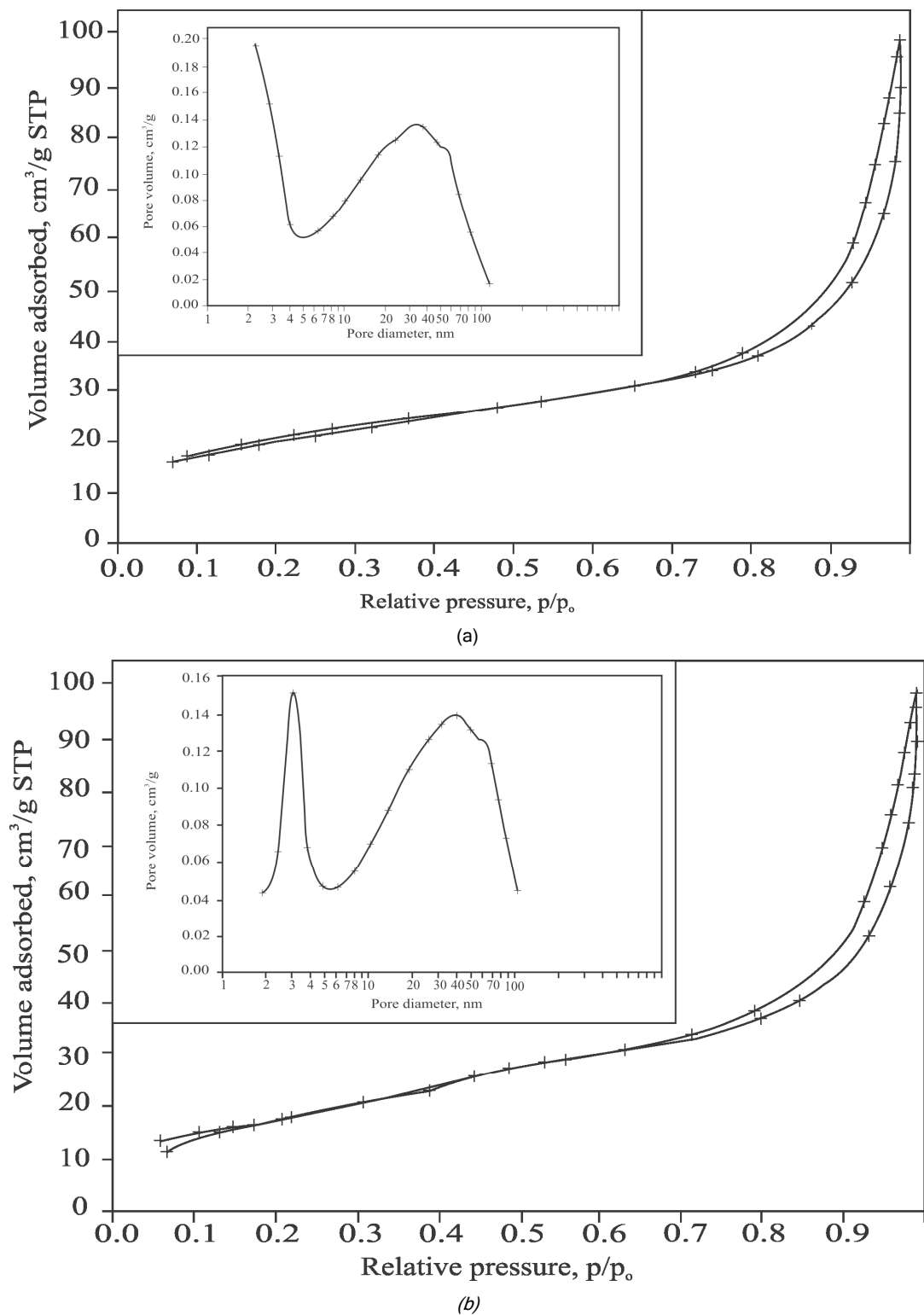


Figure 2. N_2 adsorption-desorption isotherms and pore size distribution for sulfated zirconia catalysts:
a) 4-SZrO₂-600, b) 4-SZrO₂-700.

for the catalyst 4-PhZrO₂-600 that S_{BET} exceeds 100 m²/g (Table 1). Such high specific surface area may be correlated with a bimodal pore size distribution [11,23] characterized with a substantial fraction of

mesopores also responsible for the considerable pore volume of the catalyst (0.24 cm³/g) accompanied by the presence of the small mesopores/micropores. In the earlier investigations on the phosphated zirconia,

but based on different precursor(s), it is claimed an absence of microporosity [17]. Two well defined maxima in the PSD of 30 and 3.5 nm are observed for the catalyst 4- PhZrO_2 -600 (Figure 3). This catalyst has a more pronounced maximum in the region of small mesopores of 3.5 nm.

The general feature of the catalysts texture of phosphated zirconia-based samples with the same phosphates content is the higher the calcination temperature used the smaller specific surface areas are registered. The shapes of the N_2 isotherms are of typical IV-type with a type H1 desorption hysteresis and completely comparable with the same ones of the

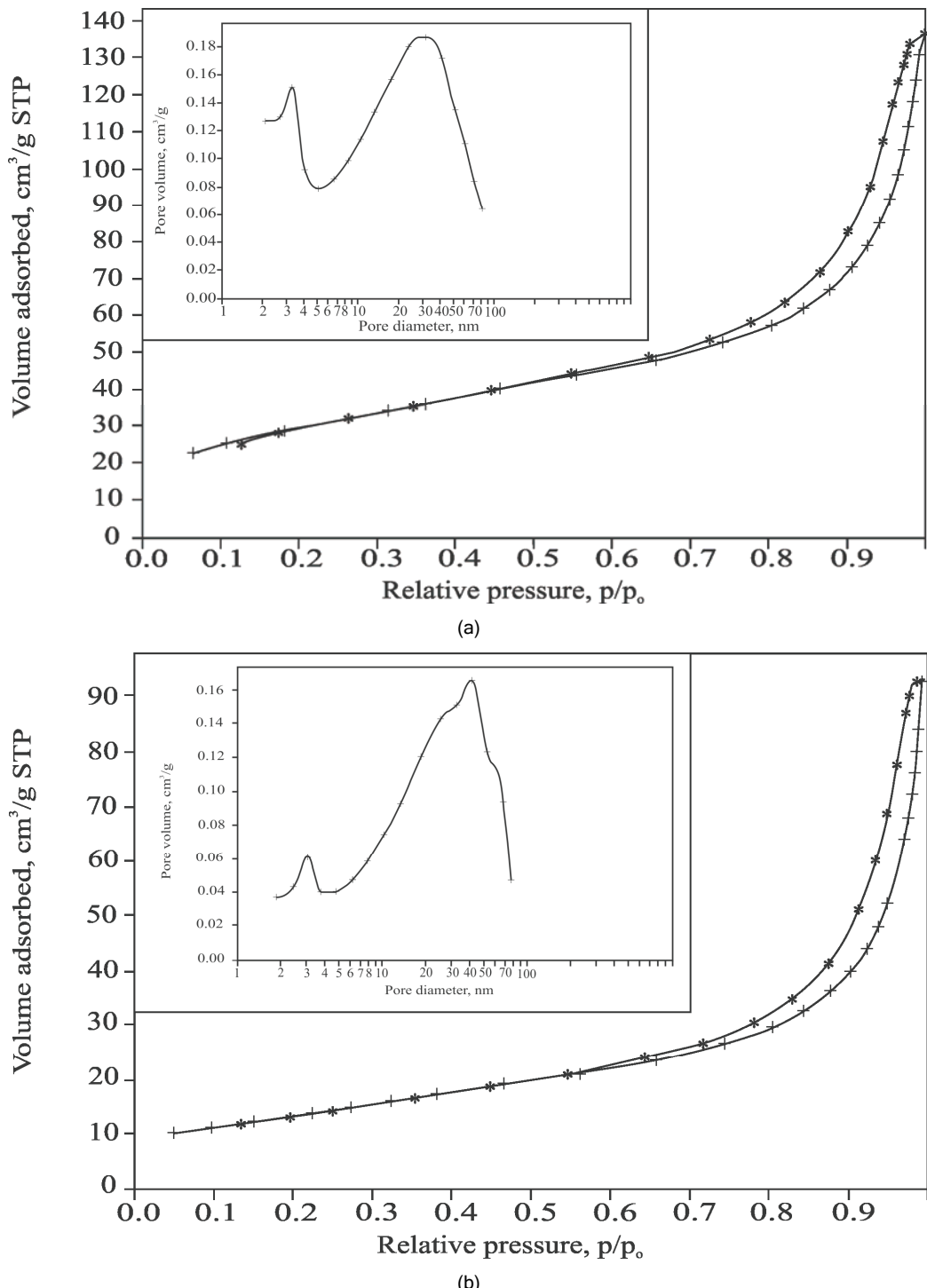


Figure 3. N_2 adsorption-desorption isotherms and pore size distribution for phosphated zirconia catalysts:
a) 4 - PhZrO_2 - 600, b) 4 - PhZrO_2 - 700.

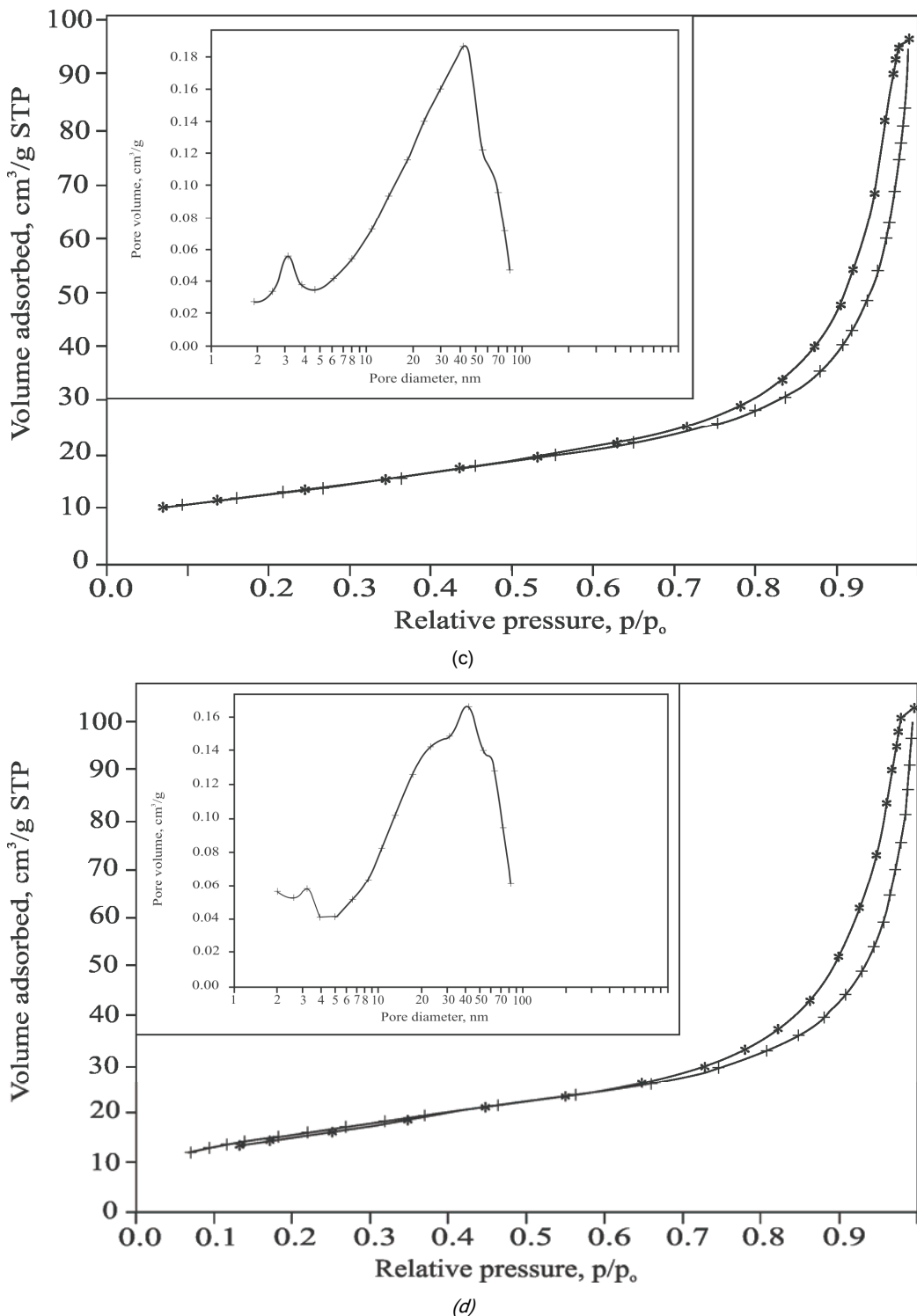


Figure 3. (Continued) N_2 adsorption-desorption isotherms and pore size distribution for phosphated zirconia catalysts:
 c) 10 - $\text{PhZrO}_2 - 600$, d) 10 - $\text{PhZrO}_2 - 700$.

sulfated catalysts (Figures 2 and 3), and with textural features of the phosphated zirconia, based on oxide and hydroxide precursors, reported previously [17]. Merely, the hysteresis for phosphated zirconia-based sample is slightly shifted to lower p/p_0 values. Accordingly, phosphated catalysts series showed some-

what narrower pore size distribution (Table 1) compared to the sulfated catalysts series. Among all samples in the phosphated catalysts series, two maxima in the PSD are observed (Figure 3), where one maximum (in the region 20-80 nm) is shifted to lower values compared to the sulfated catalysts series. In

other words, the BJH curves also showed the most populated pore radii are shifted from larger to somewhat smaller mesopores.

In general, transformation of the (meso) porous pore structure as a function of calcination temperature is predictable; the average pore diameters are increased when the calcinations temperatures are increased from 600 to 700 °C in the particular catalysts series. This is an indication on width pore broadening for all investigated catalysts samples in the series (sulfated or phosphated) regardless of the acidic additives used. Thus, coupled with the decrease in the specific surface area, usually indicates the sintering process occurring at higher temperatures.

Based on the XRD patterns, and our previously reported results [11], it is obvious that when heating from 450 to 600 and/or 700 °C (Figure 4), an amorphous phase of zirconium hydroxide transformed to well crystalline a mixture of tetragonal ($t\text{-ZrO}_2$) and monoclinic ($m\text{-ZrO}_2$) zirconia. In our case similar to the results of other authors [17,30,31] the crystallization to monoclinic ZrO_2 increases with calcination temperature.

XRD Patterns of the sulfated catalysts samples calcined at both temperatures indicated the tetragonal zirconia phase prevailed. In the higher presence of phosphate additives, the $m\text{-ZrO}_2$ peaks are partly suppressed in the XRD patterns, which are dominated by peaks due to t - and/or $c\text{-ZrO}_2$ (Figure 4).

Thus, the above results reveal that the presence of phosphate ions (10 wt. %) in Zr(OH)_4 stabilizes the

tetragonal ZrO_2 structure at 600 and 700 °C. An analogous effect is claimed by other authors [17] and occurred using additives of Ca^{2+} , Mg^{2+} , Y^{3+} and Ce^{4+} compounds [32,33]. Tetragonal zirconia phase is widely referred to as the active catalytic phase for the reaction of *n*-hexane isomerization [34,35].

In contrast, XRD patterns of the phosphated zirconia with minor content of phosphate reflected predominant $m\text{-ZrO}_2$ phase with weaker features of tetragonal phase (Figure 4). These results indicate that this treatment of crystalline ZrO_2 with 4 wt. % PO_4^{3-} does not influence the retardation of $m\text{-ZrO}_2$ crystallization at higher temperatures.

The line width for XRD peaks indicates that when tetragonal zirconia transforms to monoclinic zirconia the crystallite size increases (Table 2, Figure 4). This indicates that the average particle size of $m\text{-ZrO}_2$ is larger than that of t - and/or $c\text{-ZrO}_2$ similar to the results reported for the modified (sulfated and/or phosphated) zirconia based on different precursors by other authors [30]. All these features can be related to the sintering effect [36]. However, despite such the fact, these particles especially tetragonal ZrO_2 particles are still near critical value [37,38] reported earlier as important for the catalytic activity when sulfate additives were used. The authors impose similar behavior for phosphated zirconia based catalysts when nominal 10 wt. % of phosphates additives are applied (*i.e.*, higher than 4 wt. %) in modification. Accordingly, sulfate additives may be claimed to retard the crystallization of zirconia (into cubic and monoclinic) to occur

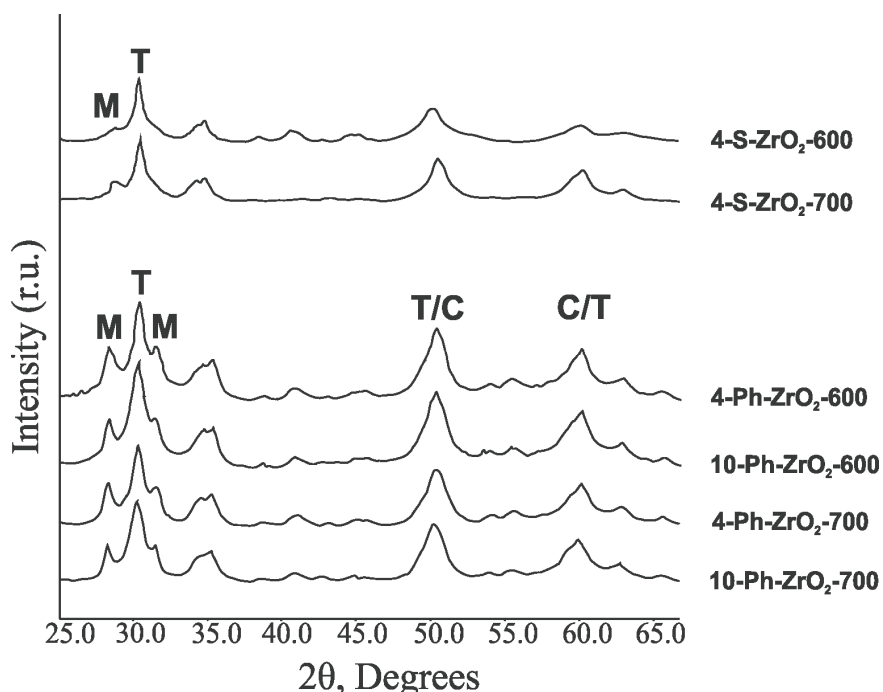


Figure 4. XRD Patterns for sulfated and phosphated zirconia based catalysts.

Table 2. Crystal phase composition, zirconia crystallite size and total acidity for sulfated and phosphated catalysts

Catalyst	Crystallite size, nm		Volume fraction of t-/m- phases, %	Acidity (H_o)
	t	m		
4 - SZrO ₂ - 600	11.7	12.1	86.7 / 13.3	$H_o < 0.8$
4 - SZrO ₂ - 700	15.0	16.4	73.1 / 26.9	$3.3 \geq H_o \gg 0.8$
4 - PhZrO ₂ - 600	13.7	13.9	48.2 / 51.8	$3.3 > H_o \gg 0.8$
4 - PhZrO ₂ - 700	18.0	18.9	47.8 / 52.2	$H_o > 3.3$
10 - PhZrO ₂ - 600	8.4	13.6	55.9 / 44.1	$3.3 > H_o \geq 0.8$
10 - PhZrO ₂ - 700	9.1	15.6	52.8 / 47.2	$3.3 \geq H_o \gg 0.8$

near 600 °C and up to 700 °C, whereas phosphate additives caused the retardation (into monoclinic phase) up to 700 °C.

It is noteworthy to stress the impact of the acidic additives on the tetragonal ZrO₂ crystallite size. Namely, sulfate additive maintained t-ZrO₂ particle size around 15 nm, but it is much more maintained (particle size < 10 nm) in phosphated zirconia with 10 wt. % of phosphates incorporated (Table 2). Therefore, taking into account catalysts structure and crystallite size, one may consider the impact of phosphates additive, but used in higher content, relatively more prominent.

Micro-crystalline oxides may have a large number of imperfections on the surface [39]. These imperfections due to oxygen and/or metal vacancies cause local/regional charge imbalances on the oxides surfaces. Hence, some authors have reported recently that the acidic properties of zirconia surface are in line with the crystallite size [40], and distribution of imperfections. The acidic properties have been reported to result in beneficial catalytic activity and selectivity.

The range of total acidity of the catalysts investigated, relative to color changes of the applied Hammett indicators, are given in Table 2. Although quite a modest range of H_o values is covered by the available indicators, all the catalysts samples, except 4-SZrO₂-600, are characterized with surface acidity within the range $3.3 \geq H_o \geq 0.8$. Namely, the catalyst 4-SZrO₂-600 exhibited higher acid strength, characterized with $H_o < 0.8$. In purpose to access more accurate acidity and/or its categorization, probes with Hammett indicators of basicity higher than that of the most basic available, crystal violet, would be required [41]. The catalyst 4-SZrO₂-600 showed the highest total acidity,

while the catalyst 4-PhZrO₂-700 impregnated with smaller nominal wt. % of phosphate and calcined at higher temperature, the lowest acidity among all the catalysts (Table 2). In general, zirconia based catalysts modified by sulfuric acid possess higher total acidity than those promoted with phosphates groups. In the case of phosphates used as acidic promoters, catalysts with higher incorporated phosphate content and calcined at lower temperatures show higher acidity. The obvious effect of calcination temperature may be related to the dynamics of acidic group removal during thermal treatment, and thus, the full amount of the remaining acidic functions after calcinations. As it is previously claimed, the resulted catalytic efficiency over sulfated zirconia based catalysts in the isomerization of *n*-hexane can be dominantly ascribed to both the total acidity and dispersion of acid sites [42]. Moreover, in the previous article on the phosphated zirconia based catalysts [43], surfaces of phosphated zirconia exposed more strong Lewis and Brønsted acid sites than pure zirconia. Therefore, here, the authors impose higher initial activities of the catalysts associated with their higher estimated acidity (Table 3).

SEM Micrographs of the selected sulfated and phosphated zirconia based catalysts are shown in Figures 5 and 6, respectively. Catalyst denoted as 4-SZrO₂-600 possesses smaller particle size (11.7 nm) than the corresponding counterpart calcined at 700 °C (particle size, 15.0 nm) in the sulfated series based on the XRD results (Table 2). General insight may be obtained from the corresponding SEM micrographs without precise estimation on the particle size. Namely, the surface morphology of the catalyst

Table 3. Initial activity and products distribution for sulfated and phosphated zirconia catalysts

Catalyst	Initial conversion, %	Hydrocarbons (HC) products distribution, %			
		Di-branched isomers	Mono-branched isomers	Cracked HC	Cyclic HC
4 - SZrO ₂ - 600	16.0	2.1	85.8	4.7	7.4
4 - SZrO ₂ - 700	12.0	1.3	88.5	4.3	5.9
4 - PhZrO ₂ - 600	0.6	1.4	84.5	7.9	6.2
10 - PhZrO ₂ - 600	1.6	4.0	88.5	0.0	7.5

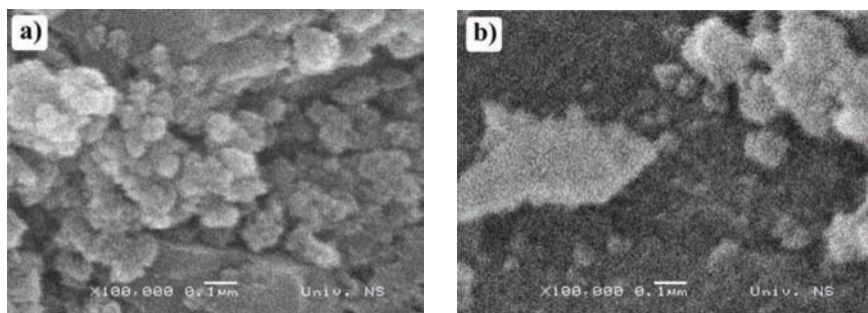


Figure 5. SEM Micrographs for sulfated zirconia catalysts: a) 4 - SZrO_2 - 600, b) 4 - SZrO_2 - 700.

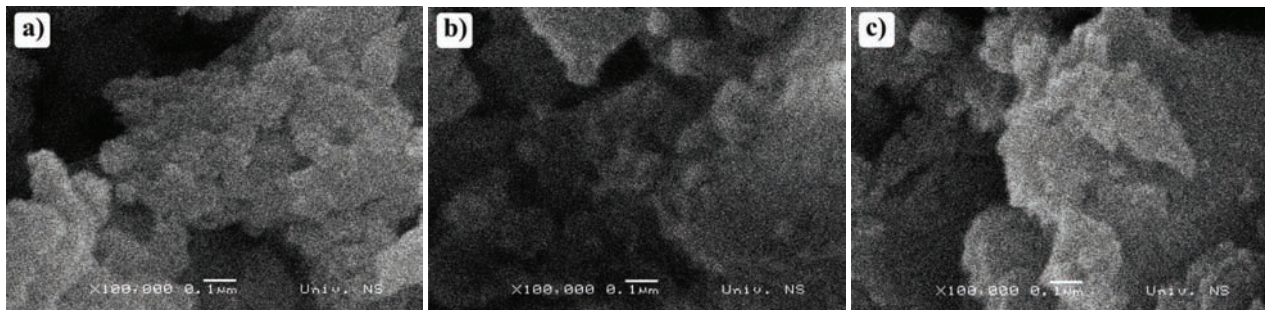


Figure 6. SEM Micrographs for phosphated zirconia catalysts: a) 4 - PhZrO_2 - 600, b) 4 - PhZrO_2 - 700, c) 10 - PhZrO_2 - 700.

$4\text{-}\text{SZrO}_2\text{-}600$ appears grainer, and consisted of particles of smaller size in contrast to the catalyst $4\text{-}\text{SZrO}_2\text{-}700$, the surface of which looks more bulky. The higher the calcination temperature used the bigger particles sizes are obtained inside the particular series of sulfated or phosphated catalysts. This is connected with the sintering process and the agglomeration of primary particles the above mentioned. The SEM characterization also supports the assumption based on the dependence of the particle size on the acidic group content [44]. Specifically, the higher phosphate amount incorporated into zirconia matrix the smaller particle size achieved under the same thermal treatment conditions applied (Figure 6). Accordingly, this observation was already proven by the XRD characterization (Table 2).

When comparing textural, structural, surface, and morphological properties of zirconia-based catalysts (sulfated and phosphated) with the exhibited catalytic efficiencies, some correlations might be imposed. Firstly, it is evident that there is a direct proportion between the fraction of the tetragonal zirconia crystal phase and catalyst activity. Secondly, the total acidity and also the surface acid strength may also play a vital role in determining the catalytic efficiency of the catalysts. Moreover, it seems that a type of acidic promoter of zirconia (sulfate or phosphate) may also contribute to increase the total acidity.

All the discussed catalysts features do not play independent roles but acting together determined the

corresponding catalytic efficiency. Here presented catalytic activity results assumed reaction runs performed in He used as carrier gas, while no activity was observed under hydrogen (Table 3). The reaction tests were carried out for as long as activity was recorded. Active catalysts based on sulfated zirconia and/or phosphated zirconia, but the latter exclusively calcined at lower temperature, exhibited the initial activities already after 5 min of the time-on-stream (TOS), and the TOS varied from 20 to 120 min in dependence on the particular catalyst sample tested. Namely, in the absence of hydrogen, a fast deactivation of the catalysts occurred due to coke accumulation and catalyst pores blocking [23].

Catalyst $4\text{-}\text{SZrO}_2\text{-}600$ showed the most favorable initial activity that can be explained by the highest total acidity and the most suitable crystal phase composition. In addition, this catalyst is characterized with high S_{BET} and appropriate porosity. Similarly, the reason for beneficial activity of the sulfated zirconia catalyst exposed to $700\text{ }^\circ\text{C}$ in calcination procedure is not only a relatively high total acidity but proper structural properties and mesoporous texture (Tables 2 and 3).

The phosphated catalysts exhibited quite low initial activity at the near edge of the experimental error. No activity or rather very low initial activity in the case of the catalyst $4\text{-}\text{PhZrO}_2\text{-}600$ is somewhat curious due to the highest S_{BET} and pore volume achieved among all catalysts investigated (Tables 2 and 3).

This fact together with acceptable total acidity ($3.3 > H_o > 0.8$), but oppositely, relatively low tetragonal crystal phase fraction for the reaction of *n*-hexane isomerization, speaks in favor of a complexity of the active phase formation in the catalyst. The mentioned finding is in agreement with the opinion of other authors [45] that reported tetragonal zirconia crystal phase as main factor influencing catalytic activity. Oppositely, here the authors suggested that structural benefit is important, but not the unique/major factor determining catalytic activity.

Poor catalytic performance of the catalyst $10 - \text{PhZrO}_2 - 600$ despite the existence of the smallest tetragonal crystallite size in the series, *i.e.*, below critical size, accompanied with the acceptable total acidity and affirmative fraction of tetragonal crystal phase reflects on the joint roles of catalyst surface, textural and structural features in determination of the final catalytic performance (Tables 2,3).

The picture of the hydrocarbons products distribution is more or less similar in the case of all the tested catalysts, regardless of the acidic promoter type. The major products are mono-branched hydrocarbons at the expense of the more desirable 2,2- and 2,3-dimethylbutanes, which indicates possible monomolecular isomerization mechanism including the carbenium ion [46]. This proposed mechanism assumed a very strong acid site(s) [44,47]. It seems that active catalytic sites of required acidity missed in the catalysts tested in the reaction runs of the present investigations.

CONCLUSIONS

Sulfated zirconia catalysts manifest more than tenfold the activity of their phosphated counterparts when calcined at lower temperature, and used in the reaction of *n*-hexane isomerization under process conditions applied. Both the type and content of acidic group incorporated into the zirconia matrix influenced the stability of the particular catalyst regarding structural properties, and crystal phase transformation from tetragonal to undesirable monoclinic one. In addition, it is observed that there is a positive relation between the fraction of the tetragonal zirconia crystal phase and catalyst activity, and that total acidity plays a vital role in determining the catalytic efficiency. Moreover, type of acidic additive should highly affect catalyst acidity, and final performance, as well.

It seems that sulfated catalysts showed favorable initial activity due to well-balanced total acidity, proper structural properties and mesoporous texture. On the other hand, quite low initial activity of the phosphated zirconia based catalyst despite the ac-

ceptable single catalytic property reflected on the complexity of the active phase formation in the catalyst. Furthermore, it is obvious that structural benefit is important, but not the major factor determining catalytic activity. Namely, there is the evident joint role of catalyst surface, textural and structural features in determination of the final catalytic performance.

Acknowledgements

The authors wish to thank to Project of Serbian Academy of Sciences and Arts, and Project ON 172061 of the Ministry of Education and Science (Republic of Serbia) for financial supports.

REFERENCES

- [1] I.E. Maxwell, J.E. Naber, K.P. De Jong, *Appl. Catal., A* **113** (1994) 153-173
- [2] J.C. Duchet, D. Guillaume, A. Monnier, C. Dujardin, J.P. Gilson, J. Van Gestel, G. Szabo, P. Nascimento, *J. Catal.* **198** (2001) 328-337
- [3] C. Jiménez, F.J. Romero, R. Roldán, J. Marinas, R. Gómez, *Appl. Catal., A* **249** (2003) 175-185
- [4] G. Boskovic, R. Micic, P. Pavlovic, P. Putanov, *Catal. Today* **65** (2001) 123-128
- [5] J.F. Allain, P. Magnoux, Ph. Schulz, M. Guisnet, *Appl. Catal. A* **152** (1997) 221-235
- [6] A. Corma, *Chem. Rev.* **95** (1995) 559-614
- [7] A.P. Bolton, in *Zeolite Chemistry and Catalysis*, J.A. Rabo (Ed.), ACS Mongr. 171, American Chemical Society, Washington, 1976, pp. 714-779
- [8] B.V. Sousa, K.D. Brito, J.J.N. Alves, M.G.F. Rodrigues, C.M.N. Yoshioka, D. Cardoso, *React. Kinet. Mech. Cat.* **102** (2011) 473-485
- [9] T. Yashima, Z.B. Wang, A. Kamo, T. Yoneda, T. Komatsu, *Catal. Today* **29** (1996) 279-283
- [10] M. Skovgaard, K. Almdal, A. van Lelieveld, *J. Mater. Sci.* **45** (2010) 6271-6274
- [11] G. Boskovic, A. Zarubica, P. Putanov, *J. Optoelect. Adv. Mater.* **7** (2007) 2251-2257
- [12] A. Zarubica, B. Jovic, A. Nikolic, P. Putanov, G. Boskovic, *J. Serb. Chem. Soc.* **74** (2009) 1429-1442
- [13] R. Suyama, T. Ashida, S. Kume, *J. Am. Ceram. Soc.* **68** (1986) 314-315
- [14] K. Föttinger, G. Kinger, H. Vinek, *Appl. Catal., A* **266** (2004) 195-202
- [15] X. Song, A. Sayari, *Catal. Rev. Sci. Eng.* **38** (1996) 329-412
- [16] N. Katada, J. Endo, K. Notsu, N. Yasunobu, N. Naito, M. Niwa, *J. Phys. Chem., B* **104** (2000) 10321-10328
- [17] G. Mekhemer, H. Ismail, *Colloids Surf., A* **164** (2000) 227-235
- [18] G. Mekhemer, *Colloids Surf., A* **141** (1998) 227-235
- [19] R. Garvie, *J. Phys. Chem.* **69** (1965) 1238-1243
- [20] Y. Zhang, X. Jin, Y. Rong, *Mater. Sci. Eng., A* **438** (2006) 399-402

- [21] C. Breitkopf, A. Garsuch, H. Papp, *Appl. Catal., A* **296** (2005) 148-156
- [22] V. Pârvulescu, S. Coman, P. Grange, V.I. Pârvulescu, *Appl. Catal., A* **176** (1999) 27-43
- [23] A. Zarubica, M. Miljkovic, E. Kiss, G. Boskovic, *Reac. Kinet. Catal. Lett.* **145** (2007) 145-150
- [24] S. Brunauer, P.H. Emmett, E. Teller, *J. Am. Chem. Soc.* **73** (1938) 309-319.
- [25] E.P. Barrett, L.G. Joyner, P.P. Halenda, *J. Am. Chem. Soc.* **73** (1951) 373-380
- [26] M.I. Zaki, Y.L. Sidrak, R.B. Fahim, *Proc. Int. Symp. Chem. Control*, Vienna, 1981, p. 155
- [27] J. Kelvin, *Phil. Mag.* **42** (1871) 488-493
- [28] K. Tanabe, *Solid Acid and Base Catalysts, Catalysis: Science and Technology*, J.R. Anderson, M. Boudart, Eds., Springer-Verlag, Berlin, 1981, pp. 231-273
- [29] G. Boskovic, A. Zarubica, M. Kovacevic, P. Putanov, *J. Therm. Anal. Cal.* **91** (2008) 849-854
- [30] A.A.M. Ali, M.I. Zaki, *Therm. Acta* **336** (1999) 17-25
- [31] A.A.M. Ali, M.I. Zaki, *Therm. Acta* **387** (2002) 29-38
- [32] R. Srinivasan, D. Taulbee, B.H. Davis, *Catal. Lett.* **9** (1999) 1-7
- [33] C.H. Perry, D.W. Liu, *J. Am. Ceram. Soc.* **68** (1985) 184-187
- [34] C. Morterra, G. Cerrato, S. Di Ciero, M. Signoretto, F. Pinna, G. Strukul, *J. Catal.* **165** (1997) 172-183
- [35] M. Signoretto, F. Pinna, G. Strukul, P. Chies, G. Cerrato, S. Di Ciero, C. Morterra, *J. Catal.* **167** (1997) 522-532
- [36] P.D.L. Mercera, J.G. Van Ommen, E.B.M. Doesburg, A.J. Burggraaf, J.R.H. Ross, *Appl. Catal.* **57** (1990) 127-148
- [37] M. Benáissa, J.G. Santiesteban, G. Díaz, C.D. Chang, M. José-Yacamán, *J. Catal.* **161** (1996) 694-703
- [38] O.V. Manoilov, R. Olindo, C.O. Areán, J.A. Lercher, *Catal. Comm.* **8** (2007) 865-870
- [39] H. Nakabayashi, N. Kakuta, A. Ueno, *Bull. Chem. Soc. Jpn.* **64** (1991) 2428-2432
- [40] T. Yamaguchi, M. Ookawa, *Catal. Today* **116** (2006) 191-195
- [41] K. Tanabe, J.R. Anderson, M. Boudart, Eds., Springer-Verlag, Berlin, 1981, pp. 231-273
- [42] A. Zarubica, P. Putanov, G. Boskovic, *Rev. Roum. Chim.* **55** (2010) 187-192
- [43] D. Spielbauer, G.A.H. Mekhemer, T. Riemer, M.I. Zaki, H. Knözinger, *J. Phys. Chem., B* **101** (1997) 4681-4688
- [44] A. Zarubica, P. Putanov, G. Boskovic, *J. Serb. Chem. Soc.* **72** (2007) 679-686
- [45] M. Signoretto, F. Pinna, G. Strukul, G. Cerrato, C. Morterra, *Catal. Lett.* **36** (1996) 129-133
- [46] T. Wakayama, H. Matsuhashi, *J. Mol. Catal., A* **239** (2005) 32-40
- [47] P.A. Jacobs, J.A. Martens, *Stud. Surf. Sci. Catal.* **58** (1991) 445-496.

N. STOJKOVIC¹
M. VASIC¹
M. MARINKOVIC¹
M. RANDJELOVIC¹
M. PURENOVIC¹
P. PUTANOV²
A. ZARUBICA¹

¹Prirodno-matematički fakultet,
Univerzitet u Nišu, Niš, Srbija
²Srpska akademija nauka i umetnosti,
Beograd, Srbija

NAUČNI RAD

UPOREDNO ISPITIVANJE IZOMERIZACIJE *n*-HEKSANA NA ČVRSTIM KISELINAMA: SULFATIMA I FOSFATIMA MODIFIKOVANOM CIRKONIJUM(IV)-OKSIDU

Sintetisane su dve serije katalizatora na bazi cirkonijum(IV)-okside modifikovanog sulfatima ili fosfatima, potom su kalcinisane na temperaturama 600 i 700 °C, i konačno testirane u reakciji izomerizacije *n*-heksana. Katalizatori sa različitim udelima sulfata ili fosfata (4 ili 10 tež. %) su karakterisani sledećim metodama/tehnikama: BET, XRD i SEM, a ukupna kiselost je испитана помоћу Hammett-ovih indikatora. Finalna katalitička svojstva su dovedena u vezu sa fizičko-hemiskim svojstvima katalizatora (površinskim, strukturalnim, teksturalnim i morfološkim). Utvrđeno je da je katalizator na bazi sulfatima modifikovanog cirkonijum(IV)-okside, kalcinisan na nižoj temperaturi, pokazao najvišu aktivnost među svim katalizatorima, što je rezultat povoljnih strukturalnih svojstava, mezoporozne teksture i visoke ukupne kiselosti. Nešto niža aktivnost katalizatora na bazi sulfonovanog cirkonijum(IV)-okside, kalcinisanog na višoj temperaturi, pripisana je delimičnom uklanjanju kiselih grupa tokom termijskog tretmana kalcinacije, time i nižom ukupnom kiselešću, i nepovoljnijim teksturalnim i strukturalnim svojstvima. Neznatna aktivnost fosfatima modifikovanog cirkonijum(IV)-okside je objašnjena nižom ukupnom kiselešću, bez obzira na kvalitet pojedinačnih katalitičkih svojstava, ukazujući na složenost nastajanja aktivne faze/centara u/na katalizatoru.

Ključne reči: katalizator; izomerizacija *n*-heksana; fosfatima modifikovan cirkonijum(IV)-oksid; sulfatima modifikovan cirkonijum(IV)-oksid.